Domain decomposition methods for electromagnetic wave propagation problems in heterogeneous media and complex domains

Victorita Dolean[1], Mohamed El Bouajaji[2], Martin J. Gander[3]
Stéphane Lanteri[2] and Ronan Perrussel[4]

[1] Laboratoire J.A. Dieudonné, CNRS UMR 6621, F-06108 Nice Cedex, France
[2] Nachos project-team, INRIA Sophia Antipolis - Méditerranée research center, F-06902 Sophia Antipolis Cedex, France - Stephane.Lanteri@inria.fr
[3] Mathematics Section, University of Geneva, CH-1211, Geneva, Switzerland
[4] Laboratoire Ampère, CNRS UMR 5005, F-69134 Ecully Cedex, France

1 Introduction

We are interested here in the numerical modeling of time-harmonic electromagnetic wave propagation problems in irregularly shaped domains and heterogeneous media. In this context, we are naturally led to consider volume discretization methods (*i.e.* finite element method) as opposed to surface discretization methods (*i.e.* boundary element method). Most of the related existing work deal with the second order form of the time-harmonic Maxwell equations discretized by a conforming finite element method [14]. More recently, discontinuous Galerkin (DG) methods have also been considered for this purpose. While the DG method keeps almost all the advantages of a conforming finite element method (large spectrum of applications, complex geometries, etc.), the DG method has other nice properties which explain the renewed interest it gains in various domains in scientific computing: easy extension to higher order interpolation (one may increase the degree of the polynomials in the whole mesh as easily as for spectral methods and this can also be done locally), no global mass matrix to invert when solving time-domain systems of partial differential equations using an explicit time discretization scheme, easy handling of complex meshes (the mesh may be a classical conforming finite element mesh, a non-conforming one or even a mesh made of various types of elements), natural treatment of discontinuous solutions and coefficient heterogeneities and nice parallelization properties. In this paper, the first order form of the time-harmonic Maxwell equations is discretized using a high order DG method formulated on unstructured simplicial meshes.

Domain decomposition (DD) methods are flexible and powerful techniques for the parallel numerical solution of systems of partial differential equations.

Their application to time-harmonic wave propagation problems began with a first algorithm proposed in [4] for solving the Helmholtz equation, and then extended and generalized for the time-harmonic Maxwell equations in [5, 3, 1]. A classical DD strategy which takes the form of a Schwarz algorithm where Després type conditions are imposed at the interfaces between neighboring subdomains was adopted in our previous work [8]. These conditions actually translate into a continuity condition for the incoming characteristic variables in the case of the first order Maxwell system. A similar approach (using Robin transmission conditions) but applied to a second order form of the Maxwell system, and in conjunction with a non-conforming finite element discretization, is presented in [13] and [18]. The analysis of a larger class of Schwarz algorithms has been performed recently in [7] where optimized transmission conditions are used. The latter extends the idea of the most general, optimized interface conditions designed for the Helmholtz problem in [12].

In this paper, we consider classical and optimized Schwarz algorithms studied in [7], in conjunction with high order DG methods [6] formulated on unstructured simplicial meshes, for the solution of the time-harmonic Maxwell equations. The rest of this paper is organized as follows. In section 2, we formulate the continuous boundary value problem to be solved. Then, in section 3, the adopted Schwarz DD method is introduced. Section 4 is devoted to the discretization of the global and domain decomposed boundary value problems. Finally, in section 5, numerical strategies for solving local problems as well as parallel computing aspects are discussed and experimental results are presented.

2 Continuous Problem

The system of normalized time-harmonic Maxwell's equations is given by:

$$\mathrm{i}\omega\varepsilon_r \boldsymbol{E} - \operatorname{curl} \boldsymbol{H} = -\boldsymbol{J}, \qquad \mathrm{i}\omega\mu_r \boldsymbol{H} + \operatorname{curl} \boldsymbol{E} = 0, \tag{1}$$

where $\boldsymbol{E}$ and $\boldsymbol{H}$ are the unknown electric and magnetic fields and $\boldsymbol{J}$ is a known current source; ε_r and μ_r respectively denote the relative electric permittivity and the relative magnetic permeability; we consider here the case of linear isotropic media. The angular frequency of the problem is given by ω. Eqs. (1) are solved in a bounded domain Ω. On the boundary $\partial\Omega = \Gamma_a \cup \Gamma_m$, the following boundary conditions are imposed:

$$\begin{aligned} &\text{- a perfect electric conductor (PEC) condition on } \Gamma_m : \boldsymbol{n} \times \boldsymbol{E} = 0, \\ &\text{- a first order absorbing condition on } \Gamma_a : \mathcal{L}(\boldsymbol{E}, \boldsymbol{H}) = \mathcal{L}(\boldsymbol{E}^{\mathrm{inc}}, \boldsymbol{H}^{\mathrm{inc}}), \end{aligned} \tag{2}$$

where $\mathcal{L}(\boldsymbol{E}, \boldsymbol{H}) = \boldsymbol{n} \times \boldsymbol{E} - Z\boldsymbol{n} \times (\boldsymbol{H} \times \boldsymbol{n})$ with $Z = \sqrt{\mu_r/\varepsilon_r}$. The vectors $\boldsymbol{E}^{\mathrm{inc}}$ and $\boldsymbol{H}^{\mathrm{inc}}$ represent the components of an incident electromagnetic wave and $\boldsymbol{n}$ denotes the unitary outward normal. Eqs. (1) and (2) can be further rewritten, assuming $\boldsymbol{J}$ equals to 0 in the form:

$$\begin{cases} \mathrm{i}\omega G_0 \boldsymbol{W} + G_x \partial_x \boldsymbol{W} + G_y \partial_y \boldsymbol{W} + G_z \partial_z \boldsymbol{W} = 0 \text{ in } \Omega, \\ (M_{\Gamma_m} - G_{\boldsymbol{n}})\boldsymbol{W} = 0 \text{ on } \Gamma_m, \\ (M_{\Gamma_a} - G_{\boldsymbol{n}})(\boldsymbol{W} - \boldsymbol{W}^{\mathrm{inc}}) = 0 \text{ on } \Gamma_a, \end{cases} \tag{3}$$

where $\boldsymbol{W} = (\boldsymbol{E}, \boldsymbol{H})^T$ is the new unknown vector and:

$$G_0 = \begin{pmatrix} \varepsilon_r \, \mathrm{I}_3 & 0_{3\times 3} \\ 0_{3\times 3} & \mu_r \, \mathrm{I}_3 \end{pmatrix}, \quad G_l = \begin{pmatrix} 0_{3\times 3} & N_{\boldsymbol{e}^l} \\ N_{\boldsymbol{e}^l}^T & 0_{3\times 3} \end{pmatrix}, \quad N_{\boldsymbol{v}} = \begin{pmatrix} 0 & v_z & -v_y \\ -v_z & 0 & v_x \\ v_y & -v_x & 0 \end{pmatrix},$$

where $(\boldsymbol{e^x}, \boldsymbol{e^y}, \boldsymbol{e^z})$ is the canonical basis of $\mathbb{R}^3$ and $\boldsymbol{v} = (v_x, v_y, v_z)^T$. The term I_3 denotes the identity matrix, and $0_{3\times 3}$ the null matrix, both of dimension 3×3. The real part of G_0 is symmetric positive definite and its imaginary part, which appears for instance in the case of conductive materials, is symmetric negative. In the following we denote by $G_{\boldsymbol{n}}$ the sum $G_x n_x + G_y n_y + G_z n_z$ and by $G^+_{\boldsymbol{n}}$ and $G^-_{\boldsymbol{n}}$ its positive and negative parts[5]. We also define $|G_{\boldsymbol{n}}| = G^+_{\boldsymbol{n}} - G^-_{\boldsymbol{n}}$. In order to take into account the boundary conditions, the matrices M_{Γ_m} and M_{Γ_a} are given:

$$M_{\Gamma_m} = \begin{pmatrix} 0_{3\times 3} & N_{\boldsymbol{n}} \\ -N_{\boldsymbol{n}}^T & 0_{3\times 3} \end{pmatrix} \quad \text{and} \quad M_{\Gamma_a} = |G_{\boldsymbol{n}}|.$$

3 A Family of Schwarz DD Algorithms

We assume that the domain Ω is decomposed into N_s subdomains $\Omega = \bigcup_{i=1}^{N_s} \Omega_i$ and let $\Gamma_{ij} = \partial\Omega_i \cap \overline{\Omega}_j$. In the following, a superscript i indicates that some notations are relative to the subdomain Ω_i and not to the whole domain Ω. We denote by $\boldsymbol{n}_{ij}$ the outward normal vector to the interface Γ_{ij}. We consider a family of Schwarz DD algorithms for solving the problem (3), given by (n denotes the Schwarz iteration):

$$\begin{cases} i\omega \, \boldsymbol{W}^{i,n+1} + \displaystyle\sum_{l\in\{x,y,z\}} G_l \partial_l \boldsymbol{W}^{i,n+1} = 0 \text{ in } \Omega_i, \\ \mathcal{B}_{\boldsymbol{n}_{ij}} \boldsymbol{W}^{i,n+1} = \mathcal{B}_{\boldsymbol{n}_{ij}} \boldsymbol{W}^{j,n} \text{ on } \Gamma_{ij}, \\ + \text{ B.C. on } \partial\Omega_i \cap \partial\Omega, \end{cases} \tag{4}$$

where the $B_{\boldsymbol{n}_{ij}}$ are interface operators. Such algorithms have been studied in detail in [7] with the aim of designing optimized overlapping and non-overlapping Schwarz methods for both the time-domain and time-harmonic Maxwell equations. Here, we consider the following situations:

- the classical Schwarz algorithm (for 2D and 3D problems) in which $\mathcal{B}_{\boldsymbol{n}_{ij}} \equiv G^-_{\boldsymbol{n}_{ij}}$,

[5] If $T\Lambda T^{-1}$ is the eigendecomposition of $G_{\boldsymbol{n}}$, then $G^{\pm}_{\boldsymbol{n}} = T\Lambda^{\pm}T^{-1}$ where Λ^+ (respectively Λ^-) only gathers the positive (respectively negative) eigenvalues.

- an optimized Schwarz algorithm (for 2D problems only) characterized by $\mathcal{B}_{\boldsymbol{n}_{ij}} \equiv G^{-}_{\boldsymbol{n}_{ij}} + \mathcal{S}_i G^{-}_{\boldsymbol{n}_{ji}}$ with $\mathcal{S}_i = \alpha_i = (i\tilde{\omega})^{-1}[p(1-i)]$ where $\tilde{\omega} = \omega\sqrt{\varepsilon\mu}$.

The optimized Schwarz algorithm selected in this study corresponds to one of several variants proposed and analyzed in [7]. In particular, in the case of a two-subdomain non-overlapping decomposition, a good choice is $p = \frac{\sqrt{C}C_{\tilde{\omega}}^{\frac{1}{4}}}{\sqrt{2}\sqrt{h}}$, which leads to the asymptotic convergence factor $\rho = 1 - \frac{\sqrt{2}C_{\tilde{\omega}}^{\frac{1}{4}}}{\sqrt{C}}\sqrt{h}$ (while $\rho = 1$ for the classical Schwarz algorithm in this configuration) where C is a constant and $C_{\tilde{\omega}} = \min(k_+^2 - \tilde{\omega}^2, \tilde{\omega}^2 - k_-^2)$ (k_- and k_+ are frequency parameters, see [7] for more details). Preliminary results of the use of this optimized Schwarz algorithm in conjunction with a high order DG method were presented in [9].

4 Discretization by a High Order DG Method

The subproblems of the Schwarz algorithm (4) are discretized using a DG formulation. In this section, we first introduce this discretization method in the one-domain case. Then we establish the discretization of the interface condition of algorithm (4) with respect to the adopted DG formulation. Let Ω_h denote a discretization of the domain Ω into a union of conforming simplicial elements K. We look for the approximate solution $\boldsymbol{W}_h$ of (3) in $V_h \times V_h$ where the functional space V_h is defined by, $V_h = \left\{\boldsymbol{U} \in [L^2(\Omega)]^3 \;/\; \forall K \in \Omega_h,\ \boldsymbol{U}_{|K} \in \mathbb{P}_p(K)\right\}$ where $\mathbb{P}_p(K)$ denotes a space of vectors with polynomial components of degree at most p over the element K.

4.1 Discretization of the One-Domain Problem

The DG discretization of system (3) yields the formulation of the discrete problem which aims at finding $\boldsymbol{W}_h$ in $V_h \times V_h$ such that:

$$
\left\{
\begin{array}{l}
\displaystyle\int_{\Omega_h} (\mathrm{i}\omega G_0 \boldsymbol{W}_h)^T \overline{\boldsymbol{V}} dv + \sum_{K\in\Omega_h} \int_K \left(\sum_{l\in\{x,y,z\}} G_l \partial_l(\boldsymbol{W}_h) \right)^T \overline{\boldsymbol{V}} dv \\
\displaystyle + \sum_{F\in\Gamma^m\cup\Gamma^a} \int_F \left(\frac{1}{2}(M_{F,K} - I_{FK} G_{\boldsymbol{n}_F}) \boldsymbol{W}_h \right)^T \overline{\boldsymbol{V}} ds \\
\displaystyle - \sum_{F\in\Gamma^0} \int_F (G_{\boldsymbol{n}_F} \mathrm{J}\boldsymbol{W}_h\mathrm{K})^T \{\overline{\boldsymbol{V}}\} ds + \sum_{F\in\Gamma^0} \int_F (S_F \mathrm{J}\boldsymbol{W}_h\mathrm{K})^T \mathrm{J}\overline{\boldsymbol{V}}\mathrm{K} ds \\
\displaystyle = \sum_{F\in\Gamma^a} \int_F \left(\frac{1}{2}(M_{F,K} - I_{FK} G_{\boldsymbol{n}_F}) \boldsymbol{W}^{\mathrm{inc}} \right)^T \overline{\boldsymbol{V}} ds, \quad \forall \boldsymbol{V} \in V_h \times V_h,
\end{array}
\right. \tag{5}
$$

where Γ^0, Γ^a and Γ^m respectively denote the set of interior (triangular) faces, the set of faces on Γ_a and the set of faces on Γ_m. The unitary normal associated to the oriented face F is $\boldsymbol{n}_F$ and I_{FK} stands for the incidence matrix between oriented faces and elements whose entries are equal to 0 if the face F does not belong to element K, 1 if $F \in K$ and their orientations match, and -1 if $F \in K$ and their orientations do not match. For $F = \partial K \cap \partial \tilde{K}$, we also define $\mathrm{J}\boldsymbol{V}\mathrm{K} = I_{FK}\boldsymbol{V}_{|K} + I_{F\tilde{K}}\boldsymbol{V}_{|\tilde{K}}$ and $\{\boldsymbol{V}\} = \frac{1}{2}\left(\boldsymbol{V}_{|K} + \boldsymbol{V}_{|\tilde{K}}\right)$. Finally, the matrix S_F, which is hermitian positive definite, permits to penalize the jump of a field or of some components of this field on the face F, and the matrix $M_{F,K}$, to be defined later, insures the asymptotic consistency with the boundary conditions of the continuous problem. Problem (5) is often interpreted in terms of local problems in each element K of Ω_h coupled by the introduction of an element boundary term called numerical flux (see also [10]). In this study, we consider two classical numerical fluxes, which lead to distinct definitions for matrices S_F and $M_{F,K}$:

- **a centered flux** (see [11] for the time-domain equivalent):

$$S_F = 0 \quad \text{and} \quad M_{F,K} = \begin{cases} I_{FK} \begin{pmatrix} 0_{3\times 3} & N_{\boldsymbol{n}_F} \\ -N^T_{\boldsymbol{n}_F} & 0_{3\times 3} \end{pmatrix} \text{ if } F \in \Gamma^m, \\ |G_{\boldsymbol{n}_F}| \text{ if } F \in \Gamma^a. \end{cases} \tag{6}$$

- **an upwind flux** (see [15, 10]):

$$S_F = \frac{1}{2} \begin{pmatrix} N_{\boldsymbol{n}_F} N^T_{\boldsymbol{n}_F} & 0_{3\times 3} \\ 0_{3\times 3} & N^T_{\boldsymbol{n}_F} N_{\boldsymbol{n}_F} \end{pmatrix},$$
$$M_{F,K} = \begin{cases} \begin{pmatrix} \frac{1}{2} N_{\boldsymbol{n}_F} N^T_{\boldsymbol{n}_F} & I_{FK} N_{\boldsymbol{n}_F} \\ -I_{FK} N^T_{\boldsymbol{n}_F} & 0_{3\times 3} \end{pmatrix} \text{ if } \in \Gamma^m, \\ |G_{\boldsymbol{n}_F}| \text{ if } F \in \Gamma^a. \end{cases} \tag{7}$$

Remark 1. The formulation of the DG scheme above (in particular, the centered and upwind fluxes) actually applies to homogeneous materials. For describing the flux in the inhomogeneous case, let us define $Z^K = \frac{1}{Y^K}$ $Z^F = \frac{Z^K + Z^{\tilde{K}}}{2}$ and $Y^F = \frac{Y^K + Y^{\tilde{K}}}{2}$ where $F = \overline{K} \cap \overline{\tilde{K}}$. With these definitions, the DG scheme in the inhomogeneous case can be written formally as (5) but by modifying S_F as:

$$S_F = \frac{1}{2} \begin{pmatrix} \frac{1}{Z^F} N_{\boldsymbol{n}_F} N^T_{\boldsymbol{n}_F} & 0_{3\times 3} \\ 0_{3\times 3} & \frac{1}{Y^F} N^T_{\boldsymbol{n}_F} N_{\mathbf{n}_F} \end{pmatrix}, \tag{8}$$

and by using for the average a weighted average $\{\cdot\}_F$ for each face F:

$$\{\mathbf{V}\}_F = \frac{1}{2}\left(\begin{pmatrix} \frac{Z^{\tilde{K}}}{Z^F} & 0_{3\times3} \\ 0_{3\times3} & \frac{Y^{\tilde{K}}}{Y^F} \end{pmatrix}\mathbf{V}_{|K} + \begin{pmatrix} \frac{Z^{K}}{Z^F} & 0_{3\times3} \\ 0_{3\times3} & \frac{Y^{K}}{Y^F} \end{pmatrix}\mathbf{V}_{|\tilde{K}}\right). \tag{9}$$

4.2 Discretization of the DD Algorithm

DG Formulation of the Multi-Domain Problem

Let Γ^{ij} denote the set of faces which belongs to $\Gamma_{ij} = \partial\Omega_i \cap \overline{\Omega}_j$. According to algorithm (4), the interface condition on Γ_{ij} is given by:

$$\mathcal{B}_{\boldsymbol{n}_{ij}}(\boldsymbol{W}^{i,n+1} - \boldsymbol{W}^{j,n}) = 0 \quad \text{for all } F \text{ belonging to } \Gamma^{ij}, \tag{10}$$

which is taken into account in a weak sense in the context of the DG formulation described in section 4.1. Then the DG discretization of a local problem of algorithm (4) can be written using (5) as:

$$\begin{cases} \text{Find } \boldsymbol{W}_h^{i,n+1} \text{ in } V_h^i \times V_h^i \text{ such that:} \\ a^i(\boldsymbol{W}_h^{i,n+1}, \boldsymbol{V}) + b^i(\boldsymbol{W}_h^{i,n+1}, \boldsymbol{V}) = f_h^i, \quad \forall \boldsymbol{V} \in V_h^i \times V_h^i, \end{cases} \tag{11}$$

with:

$$a^i(\boldsymbol{W}_h^{i,n+1}, \boldsymbol{V}) = \int_{\Omega_h^i} \left(\mathrm{i}\omega G_0 \boldsymbol{W}_h^{i,n+1}\right)^T \overline{\boldsymbol{V}} dv + \sum_{K\in\Omega_h^i} \int_K \left(\sum_{l\in\{x,y,z\}} G_l \partial_l(\boldsymbol{W}_h^{i,n+1})\right)^T \overline{\boldsymbol{V}} dv,$$

$$b^i(\boldsymbol{W}_h^{i,n+1}, \boldsymbol{V}) = \sum_{F\in\Gamma^{m,i}} \int_F \left(\frac{1}{2}(M_{F,K} - I_{FK} G_{\boldsymbol{n}_F})\boldsymbol{W}_h^{i,n+1}\right)^T \overline{\boldsymbol{V}} ds + \sum_{F\in\Gamma^{a,i}} \int_F \left(I_{FK} G^-_{\boldsymbol{n}_F} \boldsymbol{W}_h^{i,n+1}\right)^T \overline{\boldsymbol{V}} ds + \sum_{F\in\Gamma^{ij}} \int_F \left(I_{FK} \mathcal{B}_{\boldsymbol{n}_F} \boldsymbol{W}_h^{i,n+1}\right)^T \overline{\boldsymbol{V}} ds + \sum_{F\in\Gamma^{0,i}} \int_F \left[\left(S_F \mathrm{J}\boldsymbol{W}_h^{i,n+1}\mathrm{K}\right)^T \mathrm{J}\overline{\boldsymbol{V}}\mathrm{K} - \left(G_{\boldsymbol{n}_F} \mathrm{J}\boldsymbol{W}_h^{i,n+1}\mathrm{K}\right)^T \{\overline{\boldsymbol{V}}\}\right] ds,$$

$$f_h^i = \sum_{F\in\Gamma^{a,i}} \int_F \left(I_{FK} G^-_{\boldsymbol{n}_F} \boldsymbol{W}^{\mathrm{inc}}\right)^T \overline{\boldsymbol{V}} ds + \sum_{F\in\Gamma^{ij}} \int_F \left(I_{FK} \mathcal{B}_{\boldsymbol{n}_F} \boldsymbol{W}_h^{j,n}\right)^T \overline{\boldsymbol{V}} ds.$$

We note that the proposed numerical treatment of the interface condition (10) (see the boundary integral terms on Γ^{ij} in the expressions for b_i and f_h^i) is only valid for the classical interface condition or for a zero-order optimized interface condition such as the one selected in this study.

Formulation of an Interface System

In the two-domain case the Schwarz algorithm can be written formally as:

$$\begin{cases} \mathcal{L}\boldsymbol{W}^{1,n+1} = \boldsymbol{f}^1, \text{ in } \Omega_1, \\ \mathcal{B}_{\boldsymbol{n}_{12}}\boldsymbol{W}^{1,n+1} = \lambda^{1,n}, \text{ on } \Gamma_{12}, \\ + \text{ B.C. on } \partial\Omega_1 \cap \partial\Omega, \end{cases} \begin{cases} \mathcal{L}\boldsymbol{W}^{2,n+1} = \boldsymbol{f}^2, \text{ in } \Omega_2, \\ \mathcal{B}_{\boldsymbol{n}_{21}}\boldsymbol{W}^{2,n+1} = \lambda^{2,n}, \text{ on } \Gamma_{21}, \\ + \text{ B.C. on } \partial\Omega_2 \cap \partial\Omega, \end{cases} \tag{12}$$

and then:

$$\lambda^{1,n+1} = \mathcal{B}_{\boldsymbol{n}_{12}}\boldsymbol{W}^{2,n+1} \text{ on } \Gamma_{12}, \quad \lambda^{2,n+1} = \mathcal{B}_{\boldsymbol{n}_{21}}\boldsymbol{W}^{1,n+1} \text{ on } \Gamma_{21}, \tag{13}$$

where $\mathcal{L}$ is a linear differential operator and $\boldsymbol{f}^{1,2}$ denotes the right-hand sides associated to $\Omega_{1,2}$. The Schwarz algorithm (12)-(13) can be rewritten in substructured form as:

$$\lambda^{1,n+1} = \mathcal{B}_{\boldsymbol{n}_{12}}\boldsymbol{W}^2(\lambda^{2,n}, \boldsymbol{f}^2) \quad , \quad \lambda^{2,n+1} = \mathcal{B}_{\boldsymbol{n}_{21}}\boldsymbol{W}^1(\lambda^{1,n}, \boldsymbol{f}^1),$$

where $\boldsymbol{W}^j = \boldsymbol{W}^j(\lambda^j, \boldsymbol{f}^j)$ are the solutions of the local problems. By linearity of the operators involved, an iteration of the Schwarz algorithm is then $\boldsymbol{\lambda}^{n+1} = (\mathrm{Id} - \mathcal{T})\boldsymbol{\lambda}^n + \boldsymbol{d}$, which is a fixed point iteration to solve the interface system $\mathcal{T}\boldsymbol{\lambda} = \boldsymbol{d}$, where $\boldsymbol{\lambda} = (\boldsymbol{\lambda}^1, \boldsymbol{\lambda}^2)$. From the discrete point of view, the global problem on domain Ω can be written in the matrix form:

$$\begin{pmatrix} A_1 & 0 & R_{12} & 0 \\ 0 & A_2 & 0 & R_{21} \\ 0 & -B_{21} & \mathrm{I} & 0 \\ -B_{12} & 0 & 0 & \mathrm{I} \end{pmatrix} \begin{pmatrix} \boldsymbol{W}_h^1 \\ \boldsymbol{W}_h^2 \\ \boldsymbol{\lambda}_h^1 \\ \boldsymbol{\lambda}_h^2 \end{pmatrix} = \begin{pmatrix} \boldsymbol{f}_h^1 \\ \boldsymbol{f}_h^2 \\ \boldsymbol{0} \\ \boldsymbol{0} \end{pmatrix},$$

where $A_{1,2}$ are local matrices coupling only internal unknowns, $R_{12,21}$ express the coupling between internal unknowns and interface unknowns, and the subscript h denotes the discrete counterpart of a given quantity (*e.g.* $\boldsymbol{\lambda}_h^{1,2}$ are the discretized unknown vectors corresponding to $\boldsymbol{\lambda}^{1,2}$). The elimination of the internal unknowns $\boldsymbol{W}_h^{1,2}$ leads to the discrete interface problem $\mathcal{T}_h\boldsymbol{\lambda}_h = \boldsymbol{g}_h$ with:

$$\mathcal{T}_h = \begin{pmatrix} \mathrm{I} & B_{21}A_2^{-1}R_{21} \\ B_{12}A_1^{-1}R_{12} & \mathrm{I} \end{pmatrix} \quad \text{and} \quad \boldsymbol{g}_h = \begin{pmatrix} B_{21}A_2^{-1}\boldsymbol{f}_h^2 \\ B_{12}A_1^{-1}\boldsymbol{f}_h^1 \end{pmatrix},$$

where $\mathcal{T}_h$ and $\boldsymbol{g}_h$ are the discretization of $\mathcal{T}$ and $\boldsymbol{d}$. This system is then solved by a Krylov subspace method, as discussed in the following section.

5 Numerical and Performance Results

5.1 The 2D Case

We first present results for the solution of the 2D transverse magnetic Maxwell equations in the case of a heterogeneous non-conducting media:

$$\begin{cases} \mathrm{i}\omega\mu_r H_x + \dfrac{\partial E_z}{\partial y} = 0, \\ \mathrm{i}\omega\mu_r H_y - \dfrac{\partial E_z}{\partial x} = 0, \\ \mathrm{i}\omega\varepsilon_r E_z - \dfrac{\partial H_y}{\partial x} + \dfrac{\partial H_x}{\partial y} = 0. \end{cases}$$

The considered test problem is the scattering of a plane wave (F=300 MHz) by a dielectric cylinder. For that purpose, we make use of a non-uniform triangular mesh which consists of 2078 vertices and 3958 triangles (see Fig. 1 left). The relative permittivity of the inner cylinder is set to 2.25 while vacuum is assumed for the rest of the domain. We compare the solutions obtained using a DGTH-$\mathbb{P}_p$ method with $p = 1, 2, 3, 4$ (*i.e.* the approximation order p is the same for all the mesh elements) and a variable order DGTH-$\mathbb{P}_{p_K}$ method (*i.e.* p_K is the approximation order in element K). In the latter case, the approximation order is defined empirically at the element level based on the triangle area resulting in a distribution for which the number of elements with $p_K = 1, 2, 3, 4$ is respectively equal to 1495, 2037, 243 and 183 (contour lines of E_z are shown on Fig. 1 right). The interface system is solved using the BiCGStab method. The convergence of the iterative solution of the interface system is evaluated in terms of the Euclidean norm of the residual normalized to the norm of the right-hand side vector. The corresponding linear threshold has been set to $\varepsilon_i = 10^{-6}$. The subdomain problems are solved using the MUMPS optimized sparse direct solver [2].

Numerical simulations have been conducted on a cluster of 20 Intel Xeon/2.33 GHz based nodes interconnected by a high performance Myrinet network. Each node consists of a dual processor quad core board with 16 GB of shared memory. Performance results are summarized in Table 1 where N_s denotes the number of subdomains and '# iter' is the number of iterations of the BiCGStab method (the figures between brackets are the gains in the number of BiCGStab iterations between the classical and optimized Schwarz algorithms). Moreover, this table also includes the values of the L^2 error on the E_z component for the approximate solutions resulting from each algorithm. Wwe stress that the error is not reduced for increasing approximation order because, in the current implementation of the DG method, we make use of an affine transformation between the reference and the physical elements of the mesh. These results demonstrate that the simple optimized interface condition considered here (see Section 3) results in substantial reductions of the required number of BiCGStab iterations for convergence of the Schwarz algorithm. Worthwhile to note, the performance improvement increases with the approximation order in the DG method. Considering the case of the DGTH-$\mathbb{P}_{p_K}$ method and for the decomposition into $N_s = 4$ subdomains, the elapsed time of the simulation is equal to 25.8 sec and 3.6 sec for the classical and optimized Schwarz algorithms respectively.

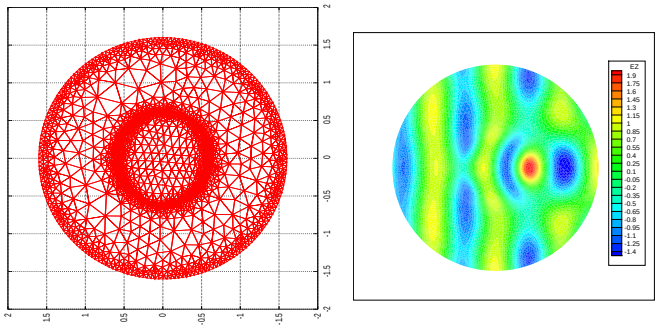

Fig. 1. Scattering of a plane wave by a dielectric cylinder. Unstructured triangular mesh (left) and contour lines of E_z (right).

Table 1. Scattering of a plane wave by a dielectric cylinder. Classical v.s. optimized Schwarz method. DGTH-$\mathbb{P}_p$ method based on the upwind flux.

Method	L^2 error on E_z Classical	L^2 error on E_z Optimized	N_s	# iter Classical	# iter Optimized
DGTH-$\mathbb{P}_1$	0.16400	0.16457	4	317	52 (6.1)
-	0.16400	0.16467	16	393	83 (4.7)
DGTH-$\mathbb{P}_2$	0.05701	0.05705	4	650	61 (10.7)
-	0.05701	0.05706	16	734	109 (6.7)
DGTH-$\mathbb{P}_3$	0.05519	0.05519	4	1067	71 (15.0)
-	0.05519	0.05519	16	1143	139 (8.2)
DGTH-$\mathbb{P}_4$	0.05428	0.05427	4	1619	83 (19.5)
-	0.05427	0.05527	16	1753	170 (10.3)
DGTH-$\mathbb{P}_{p_K}$	0.05487	0.05486	4	352	49 (7.2)
-	0.05487	0.05491	16	414	81 (5.1)

5.2 The 3D Case

We now consider a more realistic 3D problem which consists in the simulation of the exposure of a geometrical model of head tissues to a plane wave (F=1800 MHz). Starting from MR images of the Visible Human project [16], head tissues are segmented and the interfaces of a selected number of tissues (namely, the skin, the skull and the brain) are triangulated (see Fig. 2 left). Then, these triangulated surfaces are used as inputs for the generation of volume meshes. We consider here heterogeneous geometrical models involving four tissues: the skin ($\varepsilon_r = 43.85$ and $\sigma = 1.23$ S/m), the skull ($\varepsilon_r = 15.56$ and $\sigma = 0.43$ S/m), the CSF (Cerebro Spinal Fluid) ($\varepsilon_r = 67.20$ and $\sigma = 2.92$ S/m) and the brain ($\varepsilon_r = 43.55$ and $\sigma = 1.15$ S/m). Note that the exterior of the head must also be meshed, up to a certain distance from the skin, the overall domain being artificially bounded by a sphere on which

an absorbing condition is imposed. Two tetrahedral meshes have been used: the first one (referred to as M1) consists of $188,101$ vertices and $1,118,952$ tetrahedra, while the second mesh (referred to as M2) consists of $309,599$ vertices and $1,853,832$ tetrahedra. Contour lines of E_x are shown on Fig. 2 right.

Numerical simulations have been conducted on a Bull Novascale 3045 parallel system consisting of Intel Itanium 2/1.6 GHz nodes interconnected by a high performance Infiniband network. Each node consists of a 8 core board with 21 GB of shared memory. We present performance results for the classical Schwarz algorithm only and the DGTH-$\mathbb{P}_1$ discretization method. The interface system is solved using the BiCGstab(ℓ) [17] method with a linear threshold that has been set to $\varepsilon_i = 10^{-6}$. The subdomain problems are solved using the MUMPS optimized sparse direct solver [2] but this time, the L and U factors are computed in single precision arithmetic in order to reduce the memory requirements for storing the L and U factors associated subdomain problems, and an iterative refinement strategy is used to increase the accuracy of the subdomain triangular solves. Performance results are summarized in Table 2 for the factorization and solution phases. In these tables, 'RAM LU (min/max)' denotes the minimum and maximum values of the per-process memory requirement for computing and storing the L and U factors, while figures between brackets are relative parallel speedup values. We note that doubling the number of subdomains results in a slight increase in the number of BiCGstab(ℓ) iterations however, at the same time, the size of the local factors is reduced by a factor well above two and as a consequence, a super-linear speedup is observed in the solution phase.

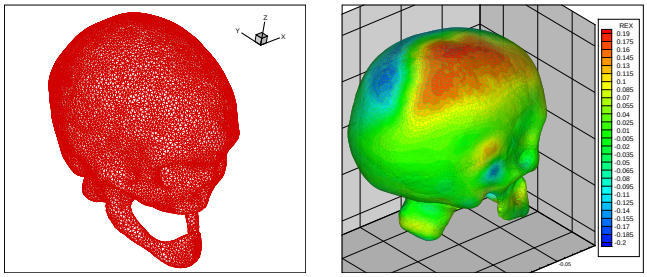

Fig. 2. Propagation of a plane wave in a heterogeneous model of head tissues. DGTH-$\mathbb{P}_1$ method based on a centered flux. Triangulated surface of the skull (left) and contour lines of E_x (right).

Table 2. Propagation of a plane wave in a heterogeneous model of head tissues. Classical Schwarz method. Performance results of the factorization and solution phases.

Mesh	# d.o.f	N_s	RAM LU (min/max)	Elapsed time LU	# iter	Elapsed time
M1	26,854,848	160	2.1 GB/3.1 GB	496 sec	30	1314 sec
-	-	320	0.8 GB/1.2 GB	132 sec (3.8)	36	528 sec (2.5)
M2	44,491,968	256	2.2 GB/3.2 GB	528 sec	42	1824 sec
-	-	512	0.8 GB/1.3 GB	142 sec (3.7)	49	785 sec (2.3)

6 Ongoing and Future Work

We have presented here some results of an ongoing collaborative effort aiming at the design of domain decomposition methods for the solution of the time-harmonic Maxwell equations modeling electromagnetic wave propagation problems in heterogeneous media and complex domains. The discretization in space of the underlying PDE model relies on a high order DG method formulated on unstructured simplicial meshes. For the solution of the resulting complex coefficients, sparse algebraic systems of equations, we consider using Schwarz algorithms in conjunction with the adopted discretization method. Future work involves the study of optimized Schwarz algorithms based on high order interface conditions for conductive media, and the design of preconditioned iterative strategies for the solution of subdomain problems.

Acknowledgment.

This work was granted access to the HPC resources of CCRT under the allocation 2009-t2009065004 made by GENCI (Grand Equipement National de Calcul Intensif).

References

[1] A. Alonso-Rodriguez and L. Gerardo-Giorda. New nonoverlapping domain decomposition methods for the harmonic Maxwell system. *SIAM J. Sci. Comput.*, 28(1):102–122, 2006.

[2] P.R. Amestoy, I.S. Duff, and J.-Y. L'Excellent. Multifrontal parallel distributed symmetric and unsymmetric solvers. *Comput. Meth. App. Mech. Engng.*, 184:501–520, 2000.

[3] P. Chevalier and F. Nataf. An OO2 (Optimized Order 2) method for the Helmholtz and Maxwell equations. In *10th International Conference on Domain Decomposition Methods in Science and in Engineering*, pages 400–407, Boulder, Colorado, USA, 1997. AMS.

[4] B. Després. Décomposition de domaine et problème de Helmholtz. *C.R. Acad. Sci. Paris*, 1(6):313–316, 1990.

[5] B. Després, P. Joly, and J.E. Roberts. A domain decomposition method for the harmonic Maxwell equations. In *Iterative methods in linear algebra*, pages 475–484, Amsterdam, 1992. North-Holland.

[6] V. Dolean, H. Fol, S. Lanteri, and R. Perrussel. Solution of the time-harmonic Maxwell equations using discontinuous Galerkin methods. *J. Comput. Appl. Math.*, 218(2):435–445, 2008.

[7] V. Dolean, L. Gerardo-Giorda, and M. Gander. Optimized Schwarz methods for Maxwell equations. *SIAM J. Scient. Comp.*, 31(3):2193–2213, 2009.

[8] V. Dolean, S. Lanteri, and R. Perrussel. A domain decomposition method for solving the three-dimensional time-harmonic Maxwell equations discretized by discontinuous Galerkin methods. *J. Comput. Phys.*, 227(3):2044–2072, 2008.

[9] V. Dolean, S. Lanteri, and R. Perrussel. Optimized Schwarz algorithms for solving time-harmonic Maxwell's equations discretized by a discontinuous Galerkin method. *IEEE. Trans. Magn.*, 44(6):954–957, 2008.

[10] A. Ern and J.-L. Guermond. Discontinuous Galerkin methods for Friedrichs systems I. General theory. *SIAM J. Numer. Anal.*, 44(2):753–778, 2006.

[11] L. Fezoui, S. Lanteri, S. Lohrengel, and S. Piperno. Convergence and stability of a discontinuous Galerkin time-domain method for the 3D heterogeneous Maxwell equations on unstructured meshes. *ESAIM: Math. Model. Numer. Anal.*, 39(6):1149–1176, 2005.

[12] M. Gander, F. Magoulès, and F. Nataf. Optimized Schwarz methods without overlap for the Helmholtz equation. *SIAM J. Sci. Comput.*, 24(1):38–60, 2002.

[13] S.C. Lee, M. Vouvakis, and J. F. Lee. A non-overlaping domain decomposition method with non-matching grids for modeling large finite antenna arrays. *J. Comput. Phys.*, 203:1–21, 2005.

[14] Peter Monk. *Finite element methods for Maxwell's equations*. Numerical Mathematics and Scientific Computation. Oxford University Press, New York, 2003.

[15] S. Piperno. L^2-stability of the upwind first order finite volume scheme for the Maxwell equations in two and three dimensions on arbitrary unstructured meshes. *M2AN: Math. Model. Numer. Anal.*, 34(1):139–158, 2000.

[16] P. Ratiu, B. Hillen, J. Glaser, and D. P. Jenkins. *Medicine Meets Virtual Reality 11 - NextMed: Health Horizon*, volume 11, chapter Visible Human 2.0 - the next generation, pages 275–281. IOS Press, 2003.

[17] G.L.G. Sleijpen and D.R. Fokkema. BiCGstab(ℓ) for linear equations involving unsymmetric matrices with complex spectrum. *Electron. Trans. Numer. Anal.*, 1:11–32 (electronic only), 1993.

[18] M. Vouvakis, Z. Cendes, and J. F. Lee. A FEM domain decomposition method for photonic and electromagnetic band gap structures. *IEEE Trans. Ant. Prop.*, 54(2):721–733, 2006.